IOPscience iopscience.iop.org

Home Search Collections Journals About Contact us My IOPscience

Nonlinear spin waves for the Heisenberg model and the ferromagnetic–antiferromagnetic bifurcations

This article has been downloaded from IOPscience. Please scroll down to see the full text article.

2004 J. Phys. A: Math. Gen. 37 8835

(http://iopscience.iop.org/0305-4470/37/37/006)

View the table of contents for this issue, or go to the journal homepage for more

Download details:
IP Address: 171.66.16.64
The article was downloaded on 02/06/2010 at 19:07

Please note that terms and conditions apply.

INSTITUTE OF PHYSICS PUBLISHING JOURNAL OF PHYSICS A: MATHEMATICAL AND GENERAL

J. Phys. A: Math. Gen. **37** (2004) 8835–8852 PII: S0305-4470(04)72783-3

Nonlinear spin waves for the Heisenberg model and the ferromagnetic–antiferromagnetic bifurcations

Leonidas Pantelidis[1]

Center for Theoretical Physics, Laboratory for Nuclear Science and Department of Physics, Massachusetts Institute of Technology, Cambridge, MA 02139, USA

E-mail: leon_pantelidis@alum.mit.edu

Received 28 November 2003
Published 1 September 2004
Online at stacks.iop.org/JPhysA/37/8835
doi:10.1088/0305-4470/37/37/006

Abstract

We present finite-amplitude spin-wave solutions for the nonlinear equations of the classical Heisenberg model on a general periodic lattice. These are families of periodic solutions bifurcating from the ferromagnetic (FR) and antiferromagnetic (AF or Néel) states which are fixed points of the flow. We allow for longitudinal anisotropy and constant uniform magnetic field in the direction of anisotropy. We find analytical expressions for the energy–frequency (e–w) curves of these families. In particular, we show that the AF families come in pairs of vertical lines. In the expression of both the FR and AF nonlinear spin waves (NLSWs), we are able to eliminate the amplitude in favour of the frequency and/or energy. All special cases of solutions are carefully analysed. We discover that the two AF families end on the FR family of a corresponding wavevector. This correspondence can be made precise without compromising the generality of the lattice. Our major point is the proof that these FR–AF intersections on the e–w plot are isochronous branchings. Hence, we establish a novel view of the AF NLSWs as bifurcations of the FR NLSWs.

PACS number: 05.45.−a

1. Introduction

The Heisenberg model (HM) has been a subject of immense interest in many-body physics for a long time. It arises as an effective quantum-spin-system theory for the complex interactions between electrons in insulating crystals [1–4], and successfully describes the *ferromagnetic* (FR) or *antiferromagnetic* (AF) ordering of ionic spin moments at low

[1] Present address: Department of Physics and Astronomy, Swarthmore College, Swarthmore, PA 19081, USA.

temperatures [3, 4]. Extensive theoretical and experimental studies[2] have been carried out on the quantum properties of the HM, including the AF ground state, magnetic correlations, phase transitions and the Haldane gap [9] in low-dimensional magnets. Recently, the discovery of high-temperature superconductivity in lamellar copper-oxides and its connection with two-dimensional and quasi-one-dimensional antiferromagnetism have sparked renewed interest in the HM (see [18] and references therein).

The quantum regime of spin systems certainly hides a few important surprises, e.g., the Haldane gap in one dimension. However, a great variety of magnetic phenomena can also be understood by the study of classical spins. Conversely, classical magnetic systems are proving ground for a variety of modern concepts in nonlinear dynamics. In particular, the nonlinear dynamics of the one-dimensional HM and some of its variants has attracted considerable attention.

In the continuum limit, the Heisenberg chain is governed by well-known equations, such as the *sine-Gordon* and *nonlinear Schrödinger* equations, which are completely integrable. Many studies are devoted to the classical and quantum aspects of solitary excitations [26–28] in these continuous models. Higher dimensional lattices have also been treated [29, 30] as well as various generalizations (e.g., see [31]). Also, large-scale magnetization dynamics have been analysed with classical methods ([32, 33], etc).

Recently, the fabrication of magnetic superlattices[3] has motivated a number of numerical investigations of solitonic and other excitations of finite discrete chains [34–36]. However, in the discrete case, even the integrability of a simple spin ring is unlikely [37], and the only known analytical solutions so far are the nonlinear spin-wave (NLSW) solutions (apart from a few limiting cases [37]).

Ferromagnetic linear spin waves (LSWs) for the HM on a general *Bravais* lattice, as well as the corresponding NLSWs, have been worked out long ago, and can be found, for example, in [38]. Antiferromagetic NLSWs for the special case of a one-dimensional isotropic HM with equal nearest neighbour interactions appeared much later in [39]. There, it is shown that the dispersion (frequency–wavevector) relation for these exact solutions is identical to the amplitude-independent dispersion of the AF LSWs.

In all these works, the FR NLSWs are presented as families of periodic solutions parametrized by the angle between an individual spin and the z-axis (the same for all spins). On the other hand, the AF NLSW families depend on two such angles (though constrained so that only one is independent), one for the odd and one for the even sublattice. Hence, the two types of families are expressed in terms of different parameters, and no particular attention is drawn towards the relationship between the FR and AF NLSWs.

In this paper, we adopt a different point of view. We consider the anisotropic HM on a general periodic lattice and in the presence of an external magnetic field, and we parametrize the family of FR NLSWs by the frequency, instead of the amplitude, of these periodic orbits. We then derive a (quadratic) energy–frequency relation (e–w plot). This allows us to to write down the FR NLSW with the energy as a parameter. Special cases are carefully treated. In the neighbourhood of the endpoints of the e–w curve, we recover the LSW solutions. For the same system, with the extra assumption of bipartiteness for the lattice, we also introduce the AF NLSWs. We find that these solutions have an energy-independent quadratic dispersion, as it has been previously shown [39] in the particular case of an isotropic Heisenberg chain. Hence, they form a pair of vertical families for each value of the wavevector.

[2] Of course, any list of publications, we could refer to here, would be largely inadequate. For some important work in the field, see [5–25] and references therein.

[3] These materials are physical realizations of lines of large (thus classical) spins.

In the expression of the AF NLSWs, we are able to eliminate the amplitudes in favour of a single parameter, namely the energy. In this way, we can easily show that the AF families, which start from the Néel state at small amplitude, have their endpoints lying exactly on the e–w curve of a FR family. The FR–AF intersection is characterized by a smooth transition between the FR and AF NLSW. In other words, we find that the two AF families branch off the FR family of a corresponding wavevector. Our proof is for the HM on an arbitrary Bravais lattice and therefore it requires a careful treatment of the relation between the lattice srtucture and the wavevector. We finally give a detailed description of the e–w plot in all different regimes of field intensity and wavevector.

Note that there are many well-known examples of bifurcations in non-integrable systems of only a few degrees of freedom, and they are fairly well understood [40]. However, for systems with a large number of degrees of freedom, bifurcations that are formally known, not only empirically observed, are scarce. In this sense, it is quite interesting to have identified the bifurcations, for any number of spins, between the families emanating from the two extrema (at zero field) of the classical spectrum.

2. The classical HM

One way to motivate the classical HM is to employ the 'cold' (or zero temperature, or pure state) time-dependent Hartree–Fock approximation (TDHF) [41] on the quantum Heisenberg Hamiltonian

$$H = -\sum_{j<l}^{\Lambda} g_{jl}\boldsymbol{S}_j \cdot \boldsymbol{S}_l - \sum_{j=1}^{\Lambda} \boldsymbol{B}_j \cdot \boldsymbol{S}_j. \tag{2.1}$$

The first term in H contains the *exchange constants*. The second term, the *Zeeman* term, assumes the presence of an external magnetic field $\boldsymbol{B}$. We can also allow for longitudinal anisotropy Δ by defining

$$\boldsymbol{S}_j \cdot \boldsymbol{S}_l \equiv \boldsymbol{S}_j^{\perp} \cdot \boldsymbol{S}_l^{\perp} + \Delta S_j^z S_l^z \equiv \left(S_j^x S_l^x + S_j^y S_l^y\right) + \Delta S_j^z S_l^z. \tag{2.2}$$

In the zero-temperature TDHF approximation, one starts with the simplifying assumption that the total wavefunction $|\Phi(t)\rangle$ of the quantum system is composed of independent particles, i.e., it is the product of single-particle wavefunctions $|\phi_j(t)\rangle$. In the case of identical fermions, the antisymmetry requirement on the wavefunction leads to the well-known Slater determinant ansatz. However, for a spin system with Λ distinguishable lattice sites, we can simply write $|\Phi(t)\rangle = \bigotimes_{j=1}^{\Lambda} |\phi_j(t)\rangle$, where all states are normalized.

The time-dependent Schrödinger equation

$$\left(\mathrm{i}\frac{\mathrm{d}}{\mathrm{d}t} - H\right)|\Phi\rangle = 0 \tag{2.3}$$

and its complex conjugate are equivalent to Dirac's action principle $\delta S = 0$ against independent variations of $\langle\Phi|$ and $|\Phi\rangle$ in

$$S[\Phi] = \int_{t_1}^{t_2} \mathrm{d}t \langle\Phi|\mathrm{i}\frac{\mathrm{d}}{\mathrm{d}t} - H|\Phi\rangle. \tag{2.4}$$

This yields a set of Λ nonlinear one-particle equations of motion

$$\mathrm{i}\frac{\mathrm{d}}{\mathrm{d}t}|\phi_j\rangle = \frac{\delta}{\delta\langle\phi_j|}\langle\Phi|H|\Phi\rangle, \qquad j = 1, \ldots, \Lambda. \tag{2.5}$$

From (2.1) the energy expectation value of the Hartree–Fock state $|\Phi\rangle$ reads

$$\mathcal{H} = \langle\Phi|H|\Phi\rangle = -\sum_{j<l}^{\Lambda} g_{jl}\langle\phi_j|\boldsymbol{S}_j|\phi_j\rangle\cdot\langle\phi_l|\boldsymbol{S}_l|\phi_l\rangle - \sum_{j=1}^{\Lambda}\boldsymbol{B}_j\cdot\langle\phi_j|\boldsymbol{S}_j|\phi_j\rangle \tag{2.6}$$

or

$$\mathcal{H} = -\sum_{j<l}^{\Lambda} g_{jl}\boldsymbol{u}_j\cdot\boldsymbol{u}_l - \sum_{j=1}^{\Lambda}\boldsymbol{B}_j\cdot\boldsymbol{u}_j \tag{2.7}$$

where $\boldsymbol{u}_j$ are the expectation values of the spins:

$$\boldsymbol{u}_j \equiv \langle\boldsymbol{S}_j\rangle \equiv \langle\Phi|\boldsymbol{S}_j|\Phi\rangle = \langle\phi_j|\boldsymbol{S}_j|\phi_j\rangle, \qquad j = 1,\ldots,\Lambda. \tag{2.8}$$

Inserting (2.6) into (2.5), we find that each spin evolves according to

$$\mathrm{i}\frac{\mathrm{d}}{\mathrm{d}t}|\phi_j\rangle = -\boldsymbol{\mathcal{F}}_j\cdot\boldsymbol{S}_j|\phi_j\rangle \tag{2.9}$$

where the *mean field* $\boldsymbol{\mathcal{F}}_j$ is

$$\boldsymbol{\mathcal{F}}_j \equiv \left\langle\sum_{l=1}^{\Lambda} g_{jl}\left(\boldsymbol{S}_l^{\perp} + \Delta S_l^z\mathbf{z}\right) + \boldsymbol{B}_j\right\rangle = \sum_{l=1}^{\Lambda} g_{jl}\left(\boldsymbol{u}_l^{\perp} + \Delta u_l^z\mathbf{z}\right) + \boldsymbol{B}_j, \tag{2.10}$$

$\mathbf{z}$ being the unit vector in the z-direction. This $\boldsymbol{\mathcal{F}}_j$ is the effective field the jth spin interacts with. Note that the motion of the approximate total wavefunction is governed by a Schrödinger equation

$$\mathrm{i}\frac{\mathrm{d}}{\mathrm{d}t}|\Phi\rangle = H_{\mathrm{HF}}|\Phi\rangle \tag{2.11}$$

where

$$H_{\mathrm{HF}} = -\sum_{j=1}^{\Lambda}\boldsymbol{\mathcal{F}}_j\cdot\boldsymbol{S}_j \tag{2.12}$$

is the TDHF quantum Hamiltonian. Of course, the physical validity of TDHF, as of any mean-field approximation, should rest less on its description of the full-lattice wavefunction than its prediction of the motion of single-site expectation values [41].

Now, starting from the Heisenberg equation for the jth spin operator

$$\frac{\mathrm{d}S_j^{\alpha}}{\mathrm{d}t} = \left[S_j^{\alpha}, H_{\mathrm{HF}}\right] = -\sum_{\beta=1}^{3}\left[S_j^{\alpha}, S_j^{\beta}\right]\boldsymbol{\mathcal{F}}_j^{\beta},$$

using the spin commutation relationships

$$\left[S_j^{\alpha}, S_l^{\beta}\right] = \mathrm{i}\delta_{jl}\epsilon_{\alpha\beta\gamma}S_j^{\gamma} \tag{2.13}$$

and taking the expectation value with respect to $|\Phi\rangle$ of both sides of the resulting equation, one derives a system of Λ coupled nonlinear equations of motion

$$\frac{\mathrm{d}\boldsymbol{u}_j}{\mathrm{d}t} = \boldsymbol{u}_j\times\underbrace{\left(\sum_{l=1}^{\Lambda} g_{jl}\left(\boldsymbol{u}_l^{\perp} + \Delta u_l^z\mathbf{z}\right) + \boldsymbol{B}_j\right)}_{\boldsymbol{\mathcal{F}}_j}, \qquad j = 1,\ldots,\Lambda \tag{2.14}$$

for the individual average spins. It is clear, from this derivation, that the cross-product (torque) form of (2.14) is due to the inner product form (2.12) of H_{HF} and is independent of

the particular expression for the mean field $\boldsymbol{\mathcal{F}}_j$. Note also that (2.14) is invariant under the rescaling transformation

$$\left(\frac{1}{t}, g, \boldsymbol{B}\right) \to J\left(\frac{1}{t}, g, \boldsymbol{B}\right) \tag{2.15}$$

where J is a real constant, hence an overall renormalization of the exchange and field strengths does not affect the dynamics.

Taking the inner product of both sides of (2.14) with $\boldsymbol{u}_j$, we see that the equations

$$u_j^2 = s_j^2, \qquad j = 1, \ldots, \Lambda, \tag{2.16}$$

with s_j arbitrary[4] non-negative real constants, are consistent with the classical dynamics. It is known that on the hypersurface defined by (2.16), one can recast (2.14) in the form of Hamilton's equations with the Hamiltonian function $\mathcal{H}$. Note finally that (2.14) is invariant under the rescaling

$$\left(\frac{1}{t}, \boldsymbol{u}_j, \boldsymbol{B}\right) \to s\left(\frac{1}{t}, \boldsymbol{u}_j, \boldsymbol{B}\right) \tag{2.17}$$

for any real constant s. Consequently, at zero magnetic field the dynamics essentially depend only on the relative (not the absolute) spin lengths.

3. Ferromagnetic NLSWs

To find the NLSW solutions, it will be more convenient to write out (2.14) in terms of the components $u_j^{\pm} \equiv u_j^x \pm \mathrm{i}u_j^y$, u_j^z:

$$\frac{\mathrm{d}u_j^+}{\mathrm{d}t} = \mathrm{i}u_j^z\left(\sum_{l=1}^{\Lambda} g_{jl}u_l^+\right) - \mathrm{i}u_j^+\left(\sum_{l=1}^{\Lambda} \Delta g_{jl}u_l^z - B\right); \qquad j = 1, \ldots, \Lambda \tag{3.1a}$$

$$2\mathrm{i}\frac{\mathrm{d}u_j^z}{\mathrm{d}t} = u_j^-\left(\sum_{l=1}^{\Lambda} g_{jl}u_l^+\right) - u_j^+\left(\sum_{l=1}^{\Lambda} g_{jl}u_l^-\right); \qquad j = 1, \ldots, \Lambda, \tag{3.1b}$$

where the magnetic field is taken to be static, homogeneous and pointing along the negative z-direction. We assume a system of Λ equal spins s, meaning that we are interested in solutions on the shell (2.16) with all s_js equal to s. The spins are sitting on the sites of a finite D-dimensional *Bravais* lattice with *Born–von–Kármán (cyclic)* boundary conditions. The exchange constants are taken as $g_{jl} = g(|\boldsymbol{R}_j - \boldsymbol{R}_l|)$, where $\boldsymbol{R}_j$ is the position vector of the j-site. Then, the interactions of an individual spin are independent of its location on the lattice.

Under these assumptions, we can easily show that the system of equations (3.1) supports finite-amplitude spin-wave solutions of the form

$$\left.\begin{cases} u_j^+ = s\sin\theta\exp[\mathrm{i}(\boldsymbol{k}\cdot\boldsymbol{R}_j + \omega t - \phi)] \\ u_j^z = s\cos\theta \end{cases}\right\} \qquad \begin{array}{ll} \theta \in [0, \pi], & \phi \in [0, 2\pi), \\ s > 0, & j = 1, \ldots, \Lambda. \end{array} \tag{3.2}$$

The wavevector $\boldsymbol{k}$ runs over a set of Λ real values that depend on the particular lattice (see section 5). As for ω, it will turn out to be a real function of $\boldsymbol{k}$. At this point though, it can be considered a general complex parameter. Note that u_j^z is a constant independent of both the

[4] If following the derivation of (2.14), the $\boldsymbol{u}_j$ adhere to their meaning as average spins, then the values of the constants s_j are actually restricted.

time t and the site j. In general, (3.2) is the only solution of the equations of motion on the equal-spins shell $u_j^2 = s^2$, with constant and equal z-components of the individual spins [42]. Let us prove first that equation (3.1b) is satisfied. When we substitute (3.2) into (3.1b), we obtain

$$0 = \sum_{l=1}^{\Lambda} g_{jl} \sin[\boldsymbol{k} \cdot (\boldsymbol{R}_l - \boldsymbol{R}_j)] \tag{3.3}$$

within a factor $2is^2 \sin^2\theta$ multiplying the sum on the right. But equation (3.3) is an identity. Indeed, due to the afore-mentioned properties of the lattice, the right-hand side of (3.3) is independent of j. Therefore, we can replace $\sum_{l=1}^{\Lambda}$ by $\frac{1}{\Lambda}\sum_{j=1}^{\Lambda}\sum_{l=1}^{\Lambda}$, which makes the validity of (3.3) obvious. As for equation (3.1a), since u_j^z in (3.2) is a constant, it becomes a first-order linear system in u_j^+. Substituting the first equation of (3.2) into (3.1a) and using (3.3), we find that, unless $\sin\theta$ is zero (corresponding to the $\theta = 0, \pi$ FR fixed points), ω needs to be related to $\boldsymbol{k}$ by an amplitude-dependent dispersion relation. That, we can write as

$$w(\boldsymbol{k}, \theta) = b + \cos\theta[1 - v(\boldsymbol{k})] \tag{3.4}$$

with the following definitions[5]:

$$J \equiv -\frac{1}{2D}\sum_{l=1}^{\Lambda} g_{jl}, \tag{3.5}$$

$2D$ being the number of neighbours of a site,

$$w \equiv \frac{\omega}{2DJ\Delta s} \tag{3.6}$$

$$b \equiv \frac{B}{2DJ\Delta s} \tag{3.7}$$

and

$$v(\boldsymbol{k}) \equiv -\frac{1}{2DJ\Delta}\sum_{l=1}^{\Lambda} g_{jl} \cos[\boldsymbol{k} \cdot (\boldsymbol{R}_l - \boldsymbol{R}_j)]. \tag{3.8}$$

Now, if $v \neq 1$, we can invert (3.4) for $\cos\theta$ and substitute in (3.2). In this way, we find an expression for the NLSWs in terms of the frequency

$$\left.\begin{cases} u_j^+ = s\left[1 - \left(\frac{w-b}{1-v}\right)^2\right]^{\frac{1}{2}} \exp[\mathrm{i}(\boldsymbol{k} \cdot \boldsymbol{R}_j + w\tau - \phi)] \\ u_j^z = s\frac{w-b}{1-v} \end{cases}\right\} \qquad \begin{array}{l} b - |1-v| \leqslant w \leqslant b + |1-v| \\ \phi \in [0, 2\pi), \quad j = 1, \ldots, \Lambda, \end{array} \tag{3.9}$$

where τ is the rescaled (dimensionless) time

$$\tau \equiv (2DJ\Delta s)t. \tag{3.10}$$

According to (2.7), the energy associated with the solution (3.2) is given by

$$e(\boldsymbol{k}, \theta) = 2b\cos\theta + \cos^2\theta + v(\boldsymbol{k})\sin^2\theta \tag{3.11}$$

where

$$e \equiv \frac{\mathcal{H}}{\Lambda DJ\Delta s^2}. \tag{3.12}$$

[5] For a D-dimensional hypercubic lattice with only nearest-neighbour interactions, $2D$ is the coordination number and so the non-vanishing exchange constants are simply $g_{jl} = -J$.

Eliminating the amplitude $\cos\theta$ between (3.4) and (3.11), one finds the quadratic e–w curves

$$e(\boldsymbol{k}, w) = v(\boldsymbol{k}) - \frac{b^2}{1 - v(\boldsymbol{k})} + \frac{1}{1 - v(\boldsymbol{k})} w^2 \tag{3.13}$$

with $\boldsymbol{k}$ labelling the different families of periodic orbits (3.9). Moreover, we can substitute $\cos\theta$ from (3.11) into (3.2) to get an energy parametrization of the families

$$\left\{\begin{array}{l} u_j^+ = s\left[\frac{1-e}{1-v} + \frac{2b}{1-v}\frac{-b\pm\sqrt{b^2+(1-v)(e-v)}}{(1-v)}\right]^{\frac{1}{2}} \\ \quad \times \exp\left[\mathrm{i}\left[\boldsymbol{k}\cdot\boldsymbol{R}_j \right.\right. \\ \quad \left.\left. \pm \tau\sqrt{b^2+(1-v)(e-v)} - \phi\right]\right] \\ u_j^z = s\frac{-b\pm\sqrt{b^2+(1-v)(e-v)}}{(1-v)} \end{array}\right\} \quad \begin{array}{l} 1-2|b| \leqslant e \leqslant 1+2|b|, \quad \text{if } |b| \geqslant |1-v| \\ v - \frac{b^2}{1-v} \leqslant e \leqslant 1+2|b|, \quad \text{if } |b| \leqslant 1-v \\ 1-2|b| \leqslant e \leqslant v - \frac{b^2}{1-v}, \quad \text{if } |b| \leqslant v-1 \\ \phi \in [0, 2\pi), \quad j = 1, \ldots, \Lambda. \end{array} \tag{3.14}$$

According to (3.9) w varies smoothly between its limits and so the double sign $\pm$ in (3.14) does not signify two different families; it is just the sign of w. The inequalities in (3.14) determine the energy range. The quickest way to derive them is by requiring that the argument of the square root in (3.14b) be non-negative and also using (3.13) in conjunction with the inequalities in (3.9). Expressions (3.9) and (3.14) describe the FR NLSW families (see figure 1) with the period and energy respectively as continuation parameters. These families consist of non-trivial periodic trajectories, plus the equilibrium point $(0, v-b^2/(1-v))$ which exists for $|b| \leqslant |1-v|$ and corresponds to the angle $\theta = \arccos[b/(v-1)]$. For $b = \pm(v-1)$, this point coincides with the FR state (all spins parallel) along the $\pm z$-axis and is the highest (lowest) energy orbit of the FR family for $v > 1 (v < 1)$.

In the special case $v = 1$, we find from (3.4) and (3.11) that (3.2) gives a vertical family with the frequency $w = b$:

$$\left\{\begin{array}{l} u_j^+ = s\left[1 - \left(\frac{e-1}{2b}\right)^2\right]^{\frac{1}{2}} \exp[\mathrm{i}(\boldsymbol{k}\cdot\boldsymbol{R}_j + b\tau - \phi)] \\ u_j^z = s\frac{e-1}{2b} \end{array}\right\} \quad \begin{array}{l} \phi \in [0, 2\pi) \\ 1-2|b| \leqslant e \leqslant 1+2|b| \\ j = 1, \ldots, \Lambda. \end{array} \tag{3.15}$$

At zero magnetic field ($b = 0$), its e–w plot collapses to the point $(0, 1)$. That limit of equation (3.15) is a family of degenerate fixed points of energy $e = 1$, which can be found by simply setting $\omega = 0$ in (3.2).

Note that at $\boldsymbol{k} = \boldsymbol{0}$ equation (3.2) gives a family of cycles that are independent of j. For $\theta \neq 0, \pi$ all spins point along the same direction as they precess about the z-axis with the dimensionless frequency

$$w = b + \cos\theta\left(1 - \frac{1}{\Delta}\right). \tag{3.16}$$

In fact, it is easy to see that these are the only spatially homogeneous solutions[6] of the equations of motion (3.1a), (3.1b). Note that at zero magnetic field, the planar $\left(\theta = \frac{\pi}{2}\right)$ solutions are stationary and particularly in the isotropic case ($\Delta = 1$) all the solutions in the family are stationary.

[6] For the general XYZ Heisenberg model and for spatially homogeneous solutions, the equations of motion for the spins are equivalent to the Euler equations of motion for the angular frequency of a torque-free rigid body [37]. The spins perform a precessional motion around one of the axes with nutation (Poinsot's motion). Here, the x–y isotropy removes the latter.

In the vicinity of the endpoints of the FR family we have $\theta \approx 0, \pi$, $w \approx b \pm (1 - v)$, $e = 1 \pm 2b$ and, to lowest order in $\sigma \equiv \sin\theta \approx 0$, the periodic trajectories are the FR linear spin waves

$$\left.\begin{cases} u_j^+ = \sigma \exp\{\mathrm{i}[\boldsymbol{k}\cdot\boldsymbol{R}_j + (b \pm (1-v))\tau - \phi]\} \\ u_j^z = \pm s \end{cases}\right\} \qquad \phi \in [0, 2\pi), \quad j = 1, \ldots, \Lambda. \tag{3.17}$$

As a closing remark for this section, note that the FR spin waves are independent of the parameters J and s. The same holds for the AF spin waves that we discuss in the following section. This is due to the rescaling symmetries (2.15) and (2.17) of the dynamics. The spin waves depend on the relative interactions between different sites (determined by D and g_{jl}), the anisotropy Δ (only through $v(\boldsymbol{k})$), the field b and finally the number of spins Λ.

4. Antiferromagnetic NLSWs

We now impose the additional requirement that the lattice is *bipartite*, that is, it is divided into two disjoint sublattices $\mathcal{A}$ and $\mathcal{B}$, so that any two interacting sites belong to different sublattices. We also maintain that interactions of a site are location independent; in particular, every spin has the same interactions irrespective of the sublattice to which it belongs. Then, we may ask whether the system of (3.1a), (3.1b) admits solutions of the type (3.2) but for each of the two sublattices separately:

$$\left.\begin{cases} u_j^+ = s \sin\theta_{\mathcal{A}(\mathcal{B})} \\ \quad \times \exp[\mathrm{i}(\boldsymbol{k}\cdot\boldsymbol{R}_j + \omega t - \phi_{\mathcal{A}(\mathcal{B})})] \\ u_j^z = s\cos\theta_{\mathcal{A}(\mathcal{B})} \end{cases}\right\} \qquad \begin{array}{l} \theta_{\mathcal{A}(\mathcal{B})} \in [0, \pi], \quad \phi_{\mathcal{A}(\mathcal{B})} \in [0, 2\pi), \\ s > 0, \quad j \in \mathcal{A}(\mathcal{B}) \subset \{1, \ldots, \Lambda\}. \end{array} \tag{4.1}$$

The wavevector $\boldsymbol{k}$ assumes $\Lambda/2$ distinct values determined by the lattice structure. The discussion here is independent of the particular values of $\boldsymbol{k}$, so we defer further details on that until section 5. In equation (4.1), it turns out that $\theta_{\mathcal{A}}$ and $\theta_{\mathcal{B}}$ are not independent and neither are $\phi_{\mathcal{A}}$ and $\phi_{\mathcal{B}}$. Yet, we will find that (4.1) provides a class of solutions broader than (3.2). In [42], it is argued that (4.1) is, in general, the only solution of the equations of motion on the equal-spins shell $u_j^2 = s^2$, and with constant and equal z-components of the individual spins in each sublattice. Substituting (4.1) in (3.1b) and (3.1a) and making use of (3.3) leads to

$$0 = v \sin\theta_{\mathcal{A}} \sin\theta_{\mathcal{B}} \sin(\phi_{\mathcal{A}} - \phi_{\mathcal{B}}) \tag{4.2}$$

and

$$\sin\theta_{\mathcal{A}}(b + \cos\theta_{\mathcal{B}} - w) = v\cos\theta_{\mathcal{A}} \sin\theta_{\mathcal{B}} \exp[\mathrm{i}(\phi_{\mathcal{A}} - \phi_{\mathcal{B}})] \tag{4.3}$$

(as well as the $\mathcal{A} \leftrightarrow \mathcal{B}$ interchange of (4.3)) respectively. We now explore the possible solutions of (4.2), (4.3).

First we consider the case where $\theta_{\mathcal{A}} = \theta_{\mathcal{B}} = \theta$. The vanishing of $\sin\theta$ satisfies (4.2), (4.3) and, according to (4.1), it corresponds to two opposite FR fixed points (spins 'up', spins 'down'). In this trivial case the phases $\phi_{\mathcal{A}}, \phi_{\mathcal{B}}$ are irrelevant. In what follows, we assume that $\sin\theta$ is different from zero. Since, in general, v does not vanish either, we are left in (4.2) with just $\sin(\phi_{\mathcal{A}} - \phi_{\mathcal{B}}) = 0$ which implies

$$\phi_{\mathcal{B}} = \phi_{\mathcal{A}} = \phi, \tag{4.4}$$

or else

$$\phi_{\mathcal{B}} - \pi = \phi_{\mathcal{A}} = \phi. \tag{4.5}$$

In the case (4.4), one re-discovers, as expected, the FR NLSWs. The same holds true for (4.5). Indeed, we will show in section 5 that for each $\boldsymbol{k}$ there is a $\widetilde{\boldsymbol{k}}$ such that

$\widetilde{\boldsymbol{k}} \cdot \boldsymbol{R}_j = \boldsymbol{k} \cdot \boldsymbol{R}_j - \phi_{\mathcal{A}(\mathcal{B})}$ and $v(\widetilde{\boldsymbol{k}}) = -v(\boldsymbol{k})$. Therefore, (4.1) and (4.3) reduce to (3.2) and (3.4) respectively for the wavevector $\widetilde{\boldsymbol{k}}$. Finally, for $\boldsymbol{k}$ such that $v = 0$ (if it exists), we again find an FR NLSW. However $\phi_{\mathcal{A}}, \phi_{\mathcal{B}}$ remain unrelated which allows for a phase difference between sublattices. This is the only solution for $\theta_{\mathcal{A}} = \theta_{\mathcal{B}} = \theta$ that is not contained in (3.2) (unless $\phi_{\mathcal{A}} = \phi_{\mathcal{B}} = \phi$).

Let us now investigate the more interesting scenario where $\theta_{\mathcal{A}} \neq \theta_{\mathcal{B}}$. Then, the solution $\sin\theta_{\mathcal{A}} = \sin\theta_{\mathcal{B}} = 0$ corresponds to two opposite Néel states (sublattice $\mathcal{A}$ 'up', sublattice $\mathcal{A}$ 'down'). In the following we assume that $\sin\theta_{\mathcal{A}} \neq 0$. If $v = 0$ the system of (4.3) and its $\mathcal{A} \leftrightarrow \mathcal{B}$ interchange imply that $\theta_{\mathcal{B}} = 0, \pi$ with $w = b \pm 1$ respectively. This means that all spins of the sublattice $\mathcal{B}$ remain aligned along the positive z-direction or the negative z-direction. Note that despite the fact that equations (4.7)–(4.11) below are derived on the assumption that v is not zero, they are consistent with the case $v = 0$. Thereby, we need not consider this case separately. For $v \neq 0$ the $\mathcal{A} \leftrightarrow \mathcal{B}$ interchange of (4.3) shows that $\sin\theta_{\mathcal{B}}$ must be different from zero, and so (4.2) yields (4.4) or (4.5). Then from equation (4.3) we obtain

$$w = b + \cos\theta_{\mathcal{B}} \mp v \cot\theta_{\mathcal{A}} \sin\theta_{\mathcal{B}}, \tag{4.6}$$

where the upper and lower signs correspond to (4.4) and (4.5) respectively. An $\mathcal{A} \leftrightarrow \mathcal{B}$ interchange in (4.6) gives for $\theta_{\mathcal{A}} \neq \theta_{\mathcal{B}}$ an additional independent equation, and these two can be solved for

$$v = \mp \frac{\sin\theta_{\mathcal{A}} \sin\theta_{\mathcal{B}}}{1 + \cos\theta_{\mathcal{A}} \cos\theta_{\mathcal{B}}} \tag{4.7}$$

and

$$w = b + \frac{\cos\theta_{\mathcal{A}} + \cos\theta_{\mathcal{B}}}{1 + \cos\theta_{\mathcal{A}} \cos\theta_{\mathcal{B}}}. \tag{4.8}$$

Apart from the double sign in front, the right-hand side of (4.7) is strictly positive. On the other hand, the sign of v is specified by its definition (3.8). Hence, if $v < 0$ the phases $\phi_{\mathcal{A}}, \phi_{\mathcal{B}}$ have to be chosen according to (4.4), while if $v > 0$ (4.5) must hold instead. Moreover, we can write (4.7) as

$$|v| = \frac{\sin\theta_{\mathcal{A}} \sin\theta_{\mathcal{B}}}{1 + \cos\theta_{\mathcal{A}} \cos\theta_{\mathcal{B}}} \tag{4.9}$$

and (4.6) as

$$w = b + \cos\theta_{\mathcal{B}} + |v| \cot\theta_{\mathcal{A}} \sin\theta_{\mathcal{B}}. \tag{4.10}$$

Comparing the squares of (4.8) and (4.9), one finds a very simple dispersion relation

$$(w - b)^2 + v^2 = 1. \tag{4.11}$$

Let us summarize the case $\theta_{\mathcal{A}} \neq \theta_{\mathcal{B}}, \sin\theta_{\mathcal{A}} \neq 0$. By inserting (4.1) into the equations of motion, we found that the phases of the sublattices satisfy (4.4) for $v > 0$ and (4.5) for $v < 0$, that is, only one phase ϕ can vary independently. We also showed that the amplitudes of the two sublattices are not unrelated, but obey the constraint (4.9). Finally we derived the quadratic amplitude-independent relation (4.11). Thus, we conclude that for any specific allowed values of $\boldsymbol{k}$ and ϕ, (4.1) describes a pair of one-parameter ($\theta_{\mathcal{A}}, \theta_{\mathcal{B}}$ are constrained) families of amplitude-independent frequencies $w = b \pm \sqrt{1 - v^2}$. We can write

$$\left.\begin{cases} u_j^+ = s\epsilon \sin\theta_{\mathcal{A}(\mathcal{B})} \\ \quad \times \exp[\mathrm{i}(\boldsymbol{k} \cdot \boldsymbol{R}_j + (b \pm \sqrt{1 - v^2})\tau - \phi)] \\ u_j^z = s \cos\theta_{\mathcal{A}(\mathcal{B})} \end{cases}\right\} \qquad \begin{array}{l} \phi \in [0, 2\pi), \quad \theta_{\mathcal{A}(\mathcal{B})} \in [0, \pi] \\ j \in \mathcal{A}(\mathcal{B}) \end{array} \tag{4.12}$$

with the definition

$$\epsilon \equiv \left\{ \begin{matrix} +1, \text{ if } v \leqslant 0 \\ \epsilon_{\mathcal{A}(\mathcal{B})}, \text{ if } v \geqslant 0 \end{matrix} \;\middle|\; \begin{matrix} \text{where} \\ \epsilon_{\mathcal{A}} \equiv -\epsilon_{\mathcal{B}} \equiv 1 \end{matrix} \right\}. \tag{4.13}$$

It is important to note that in (4.12) the angles $\theta_{\mathcal{A}}, \theta_{\mathcal{B}}$ depend on the $\pm$ sign. In fact, if $\theta_{\mathcal{A}}, \theta_{\mathcal{B}}$ are the angles corresponding to the positive sign (large frequency), then, according to (4.8), $\cos\theta_{\mathcal{A}} + \cos\theta_{\mathcal{B}}$ is non-negative, and $\pi - \theta_{\mathcal{A}}, \pi - \theta_{\mathcal{B}}$ are the angles corresponding to the negative sign (small frequency)[7]. Using (4.9), the energy (2.7) of the NLSWs (4.12) can be expressed as

$$e = b(\cos\theta_{\mathcal{A}} + \cos\theta_{\mathcal{B}}) - 1 + \frac{(\cos\theta_{\mathcal{A}} + \cos\theta_{\mathcal{B}})^2}{1 + \cos\theta_{\mathcal{A}}\cos\theta_{\mathcal{B}}}. \tag{4.14}$$

We should now analyse (4.12) in terms of the different values of v. From (4.8) we see that w is real, therefore for $\boldsymbol{k}$ such that $|v| > 1$, (4.12) is not a solution. For $|v| = 1$ there is only one family with the frequency $w = b$. From (4.8) and (4.14) we can see that the e–w plot of this family comprises a single point, $(b, -1)$, and that $\pi - \theta_{\mathcal{B}} = \theta_{\mathcal{A}} \equiv \theta$. Hence,

$$\left.\begin{matrix} u_j^+ = s\epsilon \sin\theta \exp[\mathrm{i}(\boldsymbol{k}\cdot\boldsymbol{R}_j + b\tau - \phi)] \\ u_j^z = s\epsilon_{\mathcal{A}(\mathcal{B})}\cos\theta \end{matrix}\right\} \qquad \begin{matrix} \phi \in [0, 2\pi), \quad \theta \in [0, \pi] \\ j \in \mathcal{A}(\mathcal{B}). \end{matrix} \tag{4.15}$$

Another distinct case arises at non-zero magnetic field when $|v| = \sqrt{1 - b^2}$. There are two families with frequencies $w = 0, 2b$, so the first one is a family of fixed points. Its e–w plot is just the point $(0, -1)$.

In the generic case where $|v| \in [0, 1)$ and $w \neq 0$ the system of (4.8), (4.14) can be solved for $\cos\theta_{\mathcal{A}} + \cos\theta_{\mathcal{B}}$, $\cos\theta_{\mathcal{A}}\cos\theta_{\mathcal{B}}$:

$$\cos\theta_{\mathcal{A}} + \cos\theta_{\mathcal{B}} = \frac{e+1}{w}, \qquad \cos\theta_{\mathcal{A}}\cos\theta_{\mathcal{B}} = \frac{e+1}{w(w-b)} - 1 \tag{4.16}$$

and ultimately for $\cos\theta_{\mathcal{A}}, \cos\theta_{\mathcal{B}}$ as functions of energy. In this way, we can give up the two constrained angles $\theta_{\mathcal{A}}, \theta_{\mathcal{B}}$ appearing in the expression (4.12) of the AF families, in favour of a single parameter, the energy e:

$$\left.\begin{matrix} u_j^+ = s\epsilon \left[1 - \left(\frac{e+1}{2w} \pm \epsilon_{\mathcal{A}(\mathcal{B})} \sqrt{\left(\frac{e+1}{2w}\right)^2 - \frac{e+1}{w(w-b)} + 1} \right)^2 \right]^{\frac{1}{2}} \\ \quad \times \exp[\mathrm{i}(\boldsymbol{k}\cdot\boldsymbol{R}_j + w\tau - \phi)] \\ u_j^z = s \left(\frac{e+1}{2w} \pm \epsilon_{\mathcal{A}(\mathcal{B})} \sqrt{\left(\frac{e+1}{2w}\right)^2 - \frac{e+1}{w(w-b)} + 1} \right) \end{matrix}\right\} \qquad \begin{matrix} \phi \in [0, 2\pi), \quad j \in \mathcal{A}(\mathcal{B}) \\ |v| \in [0, 1) \\ w = b \pm \sqrt{1 - v^2} \neq 0 \\ 0 \leqslant \frac{e+1}{2w(w-b)} \leqslant \frac{1}{1+|v|} \end{matrix} \tag{4.17}$$

For each value of $\boldsymbol{k}$ and ϕ, the e–w plot in this generic case consists of a pair of vertical families with the frequencies $w = b \pm \sqrt{1 - v^2}$ as indicated in (4.17). As $|v| \to 1$ from below, the two families collapse into the point $(b, -1)$ that represents the family given by (4.15). In (4.17), the double sign $\pm$ is the same for all j, but otherwise it can be chosen arbitrarily and independently for the large and the small frequency. The meaning of this sign will become clear shortly. Regarding the inequality in (4.17), the easiest way to derive it is by requiring that the argument of the square root in the expression for u_j^z be non-negative and

[7] We distinguish between small and large frequency in the rather counter-intuitive sense of algebraic value as opposed to absolute value.

also that $\frac{|u_j^z|}{s} \leqslant 1$. The energy range specified by this inequality is written more explicitly as

$$\left.\begin{aligned} &-1 \leqslant e \leqslant e_+, \quad \text{if } b \geqslant -\sqrt{1-v^2} \\ &e_+ \leqslant e \leqslant -1, \quad \text{if } b \leqslant -\sqrt{1-v^2} \end{aligned}\right\}, \qquad \text{for } w = b + \sqrt{1-v^2}$$
$$\left.\begin{aligned} &-1 \leqslant e \leqslant e_-, \quad \text{if } b \leqslant +\sqrt{1-v^2} \\ &e_- \leqslant e \leqslant -1, \quad \text{if } b \geqslant +\sqrt{1-v^2} \end{aligned}\right\}, \qquad \text{for } w = b - \sqrt{1-v^2} \tag{4.18}$$

where $e_\pm \equiv 1 - 2|v| \pm 2b\sqrt{\frac{1-|v|}{1+|v|}}$.

From (4.16) we see that the point $e = -1$ corresponds to the Néel state. To the lowest order in $\sigma \equiv s\sqrt{\frac{e+1}{w(w-b)}}$, the periodic orbits (4.17) reduce to the AF linear spin waves

$$\left\{\begin{aligned} u_j^+ &= \sigma\epsilon[1 - (\pm\epsilon_{\mathcal{A}(\mathcal{B})})(w-b)]^{\frac{1}{2}} \\ &\quad \times \exp[\mathrm{i}(\boldsymbol{k}\cdot\boldsymbol{R}_j + w\tau - \phi)] \\ u_j^z &= s(\pm\epsilon_{\mathcal{A}(\mathcal{B})}) \end{aligned}\right\} \qquad \begin{aligned} &\phi \in [0, 2\pi), \quad j \in \mathcal{A}(\mathcal{B}) \\ &w = b \pm \sqrt{1-v^2}. \end{aligned} \tag{4.19}$$

We deduce from (4.19), that the plus (minus) sign in (4.17) corresponds to sublattice $\mathcal{A}$ being 'up' ('down') at the Néel state. Note finally that (4.18) implies: $e \in [-1, e_\pm]$, if $|b| \leqslant \sqrt{1-v^2}$. Therefore, the Néel state persists as the lowest-energy point of the AF NLSW family even at non-zero, albeit not too large, external magnetic field.

5. Lattice structure and wavevector

To understand the FR–AF bifurcations described in section 6, we first need to look closer at the meaning of the wavevector $\boldsymbol{k}$ in conjunction with the lattice structure. In particular, we will show that, (4.12) and (4.17) yield distinct families of periodic trajectories only for $\Lambda/2$ values of $\boldsymbol{k}$ which we can choose so that $v(\boldsymbol{k})$ takes only non-negative (or non-positive) values.

The finite lattice is defined in terms of a *primitive* basis $\{\boldsymbol{e}_i : i = 1, \ldots, D\}$ as $\left\{\boldsymbol{R} = \sum_{i=1}^D \mu_i \boldsymbol{e}_i : \mu_i \in \{0, \ldots, L_i - 1\}, \forall i\right\}$, where L_i are integers and $\prod_{i=1}^D L_i = \Lambda$ is the total number of sites. Its *dual* basis $\{\boldsymbol{\varepsilon}_i : i = 1, \ldots, D\}$, $\boldsymbol{e}_i \cdot \boldsymbol{\varepsilon}_j = \delta_{ij}$, generates the *reciprocal* lattice $\left\{\boldsymbol{G} = \sum_{i=1}^D 2\pi\mu_i\boldsymbol{\varepsilon}_i : \mu_i \in \{0, \ldots, L_i - 1\}, \forall i\right\}$. Since $\boldsymbol{R}$ is a lattice vector, we can still get all different solutions described by (3.2) and (4.1) if we restrict $\boldsymbol{k}$ in the primitive cell $\left\{\boldsymbol{k} = \sum_{i=1}^D c_i\boldsymbol{\varepsilon}_i : c_i \in (-\pi, \pi], \forall i\right\}$ of the reciprocal lattice, (or alternatively, the first Brillouin zone). On top of this, the cyclic boundary conditions $\boldsymbol{R} \equiv \boldsymbol{R} + L_i\boldsymbol{e}_i$ give $\mathrm{e}^{\mathrm{i}\boldsymbol{k}\cdot(L_i\boldsymbol{e}_i)} = 1$ or $\mathrm{e}^{\mathrm{i}c_iL_i} = 1$. Hence, the wavevector $\boldsymbol{k}$ can only run over the Λ distinct values of the subset

$$\Sigma \equiv \left\{\boldsymbol{k} = \sum_{i=1}^D \frac{2\pi\alpha_i}{L_i}\boldsymbol{\varepsilon}_i : \alpha_i \in \left\{\left[-\frac{L_i}{2}\right] + 1, \ldots, \left[\frac{L_i}{2}\right]\right\}\right\} \tag{5.1}$$

of the reciprocal primitive cell, where $[\cdots]$ denotes the integer part. Of course, in the infinite-lattice limit ($L_i \to \infty, \forall i$), Σ coincides with the reciprocal primitive cell. When dealing with a finite block of the lattice, the defining basis $\{\boldsymbol{e}_i\}$ is singled out by the simplicity the boundary conditions attain in this basis: $j_i \equiv j_i + L_i$. However, it is a well-known fact that the choice of primitive vectors is not unique.

If the lattice is bipartite, we will show that there is always a primitive basis such that the number $|\mu| \equiv \sum_{i=1}^D \mu_i$ is even, if $\boldsymbol{R}$ belongs to the sublattice $\mathcal{A}$, and odd, if $\boldsymbol{R}$ belongs to the sublattice $\mathcal{B}$. Note first that if two successive sites along the direction of a primitive

vector $\boldsymbol{e}_i$ belong to the sublattice $\mathcal{A}$, then since $\mathcal{A}$ itself is a Bravais lattice, all sites along $\boldsymbol{e}_i$ belong to this sublattice. Moreover, there exists at least one primitive direction along which the sites of $\mathcal{A}$ and $\mathcal{B}$ are intercalated, otherwise $\mathcal{A}$ would coincide with the whole lattice. Consequently, a primitive basis with its origin on an $\mathcal{A}$ site can always be written (within a permutation of its vectors) as

$$\mathcal{P} \equiv \{\boldsymbol{e}_1, \ldots, \boldsymbol{e}_n, \boldsymbol{e}_{n+1}, \ldots, \boldsymbol{e}_D\} \qquad \text{with } 1 \leqslant n \leqslant D, \tag{5.2}$$

where the vectors $\boldsymbol{e}_1, \ldots, \boldsymbol{e}_n$ point along directions of alternating $\mathcal{A}$ and $\mathcal{B}$ sites ($\mathcal{AB}$ vectors) while all sites along the vectors $\boldsymbol{e}_{n+1}, \ldots, \boldsymbol{e}_D$ are in $\mathcal{A}$ ($\mathcal{AA}$ vectors). Parenthetically, note that for a finite lattice each dimension L_i may be either even or odd, if $i \in \{n+1, \ldots, D\}$, however if $i \in \{1, \ldots, n\} L_i$ can only be even because of the cyclic boundary conditions. Since $n \geqslant 1$, we see that the total number of sites Λ, being the product of all L_is, must also be even. We now construct the vectors

$$\mathbf{e}'_m \equiv \boldsymbol{e}_m + \sum_{i=1}^{n} l_i^{(m)} \boldsymbol{e}_i, \qquad m = n+1, \ldots, D, \tag{5.3}$$

where $l_i^{(m)}$ are integers. Any vector in $\mathcal{P}$ can clearly be expressed as an integral linear combination of vectors in the set $\mathcal{P}_a \equiv \{\boldsymbol{e}_1, \ldots, \boldsymbol{e}_n, \boldsymbol{e}'_{n+1}, \ldots, \boldsymbol{e}'_D\}$ and vice versa, so $\mathcal{P}_a$ is also a primitive basis. However, for $\sum_{i=1}^{n} l_i^{(m)}$ odd, $\mathcal{P}_a$ has the additional feature that all its vectors lie along directions of alternating $\mathcal{A}$ and $\mathcal{B}$ sites. Then in the basis $\mathcal{P}_a$, the number $|\mu|$ is even for an $\mathcal{A}$ site and odd for a $\mathcal{B}$ site. In the following we refer to a basis with this property as an $\mathcal{AB}$ basis. Note that apart from the requirement that $\sum_{i=1}^{n} l_i^{(m)}$ be odd, the integers $l_i^{(m)}$ are arbitrary. Also, one can repeat the above construction for different initial bases $\mathcal{P}$. Thus we have actually demonstrated the existence of a plurality of (countable) infinities of primitive bases with the desired 'even–odd' property for the sublattices.

Now, let the basis $\mathcal{P}$ in (5.2) be the defining basis of a finite bipartite lattice and $\mathcal{P}' = \{\boldsymbol{e}'_1, \ldots, \boldsymbol{e}'_D\}$ an arbitrary $\mathcal{AB}$ basis of the same lattice (not necessarily of the type $\mathcal{P}_a$). The change-of-basis matrix $Q, \boldsymbol{e}_i = \sum_{n=1}^{D} Q_{\mathrm{in}} \boldsymbol{e}'_n$, that also relates the reciprocal bases, $\boldsymbol{\varepsilon}'_n = \sum_{i=1}^{D} Q_{\mathrm{in}} \boldsymbol{\varepsilon}_i$, is such that both Q and its inverse Q^{-1} have integral entries. If μ_i and μ'_i are the components of a site $\boldsymbol{R}$ in $\mathcal{P}$ and $\mathcal{P}'$ respectively, then $\mu'_n = \sum_{i=1}^{D} Q_{\mathrm{in}} \mu_i$. The index $\epsilon_{\mathcal{A}(\mathcal{B})}$ introduced in (4.12) is written as

$$\epsilon_{\mathcal{A}(\mathcal{B})} = (-1)^{|\mu'|} = \exp\left(\mathrm{i}\pi \sum_{n=1}^{D} \mu'_n\right) = \exp\left[\mathrm{i} \sum_{i=1}^{D} \left(\pi \sum_{n=1}^{D} Q_{\mathrm{in}}\right) \mu_i\right] = \exp(\mathrm{i}\boldsymbol{q} \cdot \boldsymbol{R}), \tag{5.4}$$

where the components of the vector $\boldsymbol{q}$ in the reciprocal basis $\{\boldsymbol{\varepsilon}_i\}$ are

$$q_i = \pi \sum_{n=1}^{D} Q_{\mathrm{in}} + 2\pi m_i, \qquad m_i \in \mathbb{Z}. \tag{5.5}$$

For two different sites $\boldsymbol{R}_j = \sum_{i=1}^{D} \mu_i \boldsymbol{e}_i$ and $\boldsymbol{R}_l = \sum_{i=1}^{D} \nu_i \boldsymbol{e}_i$, one can see from (5.4) that $\boldsymbol{q} \cdot (\boldsymbol{R}_l - \boldsymbol{R}_j) = \pi \sum_{n=1}^{D} (\nu'_i - \mu'_i)$. This shows that if these two sites belong to different sublattices then $\boldsymbol{q} \cdot (\boldsymbol{R}_l - \boldsymbol{R}_j)$ is an odd multiple of π. Therefore, from the definition (3.8) we have that for any $\boldsymbol{k}$,

$$v(\boldsymbol{k} + \boldsymbol{q}) = -v(\boldsymbol{k}). \tag{5.6}$$

By properly choosing the integers m_i in (5.5), we introduce within the primitive cell of the reciprocal lattice the bijective (1–1 and onto) map

$$\Sigma \ni \sum_{i=1}^{D} k_i \boldsymbol{e}_i = \boldsymbol{k} \longrightarrow \widetilde{\boldsymbol{k}} \equiv \boldsymbol{k} + \boldsymbol{q} = \sum_{i=1}^{D} \left\{ k_i + \epsilon_i \pi \left[\left(\sum_{n=1}^{D} Q_{\mathrm{in}} \right) \bmod 2 \right] \right\} \boldsymbol{e}_i \in \Sigma, \tag{5.7}$$

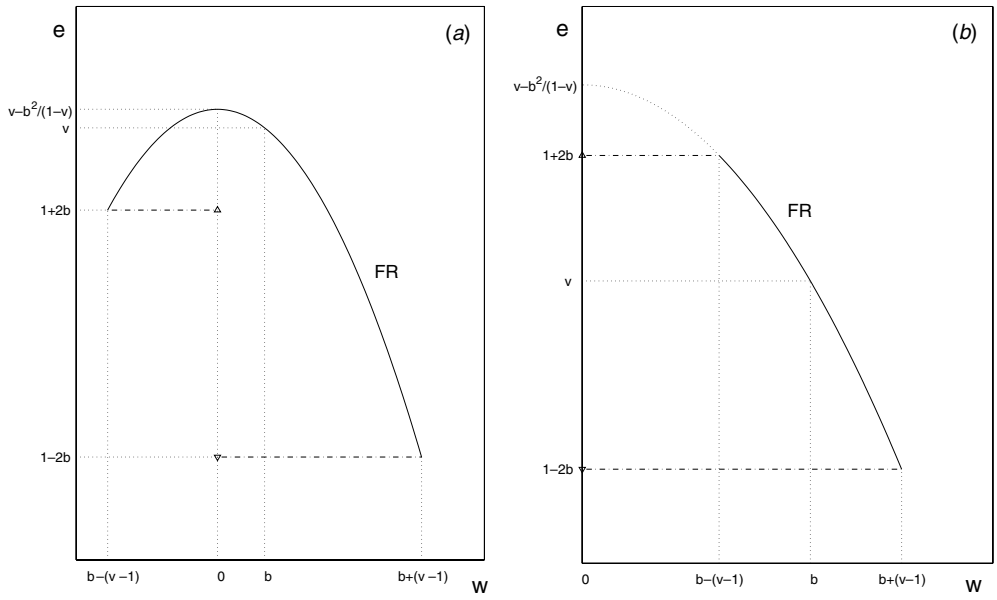

Figure 1. e–w plots of the NLSW solutions for $v > 1$ and $b > 0$. The FR fixed point with all spins pointing along the positive (negative) z-axis is denoted by $\triangle$ ($\triangledown$). The solid line is the e–w curve. The dashed-dotted lines signify bifurcations from fixed points. The dotted lines are there for the purpose of only locating certain points on the e–w curve. (a) $0 < b < v - 1$ (b) $0 < v - 1 < b$.

in which

$$\epsilon_i \equiv \begin{Bmatrix} +1, & \text{if } k_i \leqslant 0 \\ -1, & \text{if } k_i > 0 \end{Bmatrix}. \tag{5.8}$$

This map establishes a duality in the sense that $\widetilde{\widetilde{\boldsymbol{k}}} = \boldsymbol{k}$. Moreover, there are no self-dual wavevectors, that is, $\widetilde{\boldsymbol{k}} \neq \boldsymbol{k}$ for every $\boldsymbol{k} \in \Sigma$, since, according to (5.7)

$$\widetilde{k}_i = \begin{Bmatrix} k_i + \epsilon_i \pi, & \text{if } \boldsymbol{e}_i \text{ along an } \mathcal{AB} \text{ direction} \\ k_i, & \text{if } \boldsymbol{e}_i \text{ along an } \mathcal{AA} \text{ direction} \end{Bmatrix} \tag{5.9}$$

and there is at least one basis vector $\boldsymbol{e}_i$ along an $\mathcal{AB}$ direction. Consequently, the discrete primitive cell Σ is partitioned, via the bijection (5.7), into $\Lambda/2$ dual pairs $(\boldsymbol{k}, \widetilde{\boldsymbol{k}})$ of distinct wavevectors.

The highest point of the argument is this: armed with (5.4) and (5.6), one immediately realizes that families of cycles in (4.12) (or (4.17)) corresponding to dual wavevectors are identical. Hence, there are only $\Lambda/2$ distinct pairs of AF families in (4.12) (or (4.17)) (modulo the phase ϕ) labelled by $\Lambda/2$ pairwise non-dual wavevectors. It also follows from (5.6) that these $\Lambda/2$ wavevectors $\boldsymbol{k}$ can be chosen so that $v(\boldsymbol{k}) \geqslant 0$ for all $\boldsymbol{k}$, or $v(\boldsymbol{k}) \leqslant 0$ for all $\boldsymbol{k}$.

6. FR–AF bifurcations

In figure 1 we show the e–w plot of the NLSW families for a given value $v \geqslant 1$ and different regimes of the dimensionless field b. According to the discussion in section 4, this

plot contains only the FR family. From (3.13) and (3.9), we see that we can find the FR family for $v \leqslant 1$ (concave up) by reflecting, with respect to the horizontal axis $e = 1$, the FR family corresponding to $v' \geqslant 1$ (concave down) such that $v' - 1 = 1 - v$. However, for $-1 \leqslant v \leqslant 1$ the two AF families also appear and, particularly if $-1 \leqslant v \leqslant 0$ (see figure 2), their frequencies $b \pm \sqrt{1 - v^2}$ lie within the frequency domain $[b - |1 - v|, b + |1 - v|]$ (see (3.9) of the FR family. It is interesting that all e–w curves are characterized solely by the values of v and b and do not explicitly depend on any other parameters, e.g., the exchange constants, the wavevector, the anisotropy, or the number of spins. In figures 1 and 2, we have taken b to be positive. Reflecting the e–w plot with respect to the vertical axis $w = 0$ yields the e–w plot for the field $-b$. Note now that, as long as $-1 \leqslant v \leqslant 0$, any AF family with $v' = \pm v$ ends exactly on any FR family corresponding to v. Let $\boldsymbol{k}$ and $\boldsymbol{k}'$ respectively be the wavevectors of the FR family and the pair of AF families (of frequencies $b \pm \sqrt{1 - v^2}$) such that $-|v(\boldsymbol{k}')| = v(\boldsymbol{k}) \in [-1, 0]$. As we will see below, choosing these wavevectors in a simple way guarantees that the FR–AF transitions at the FR–AF intersection points are continuous. Thus, we can view the AF families as bifurcations of FR families with v from the interval $[-1, 0]$.

To prove this statement, let us first substitute the AF frequencies $w = b \pm \sqrt{1 - v^2}$, where $v^2 = v'^2$, into (3.9) to find the FR periodic orbits at the FR–AF intersection points:

$$\left.\begin{cases} u_j^+ = s\left(\frac{2v}{v-1}\right)^{\frac{1}{2}} \exp\left[\mathrm{i}\left(\boldsymbol{k}\cdot\boldsymbol{R}_j + \left(b \pm \sqrt{1-v^2}\right)\tau - \phi\right)\right] \\ u_j^z = \pm s\left(\frac{1+v}{1-v}\right)^{\frac{1}{2}} \end{cases}\right\} \qquad \begin{matrix} \phi \in [0, 2\pi) \\ v \in [-1, 0] \\ j = 1, \ldots, \Lambda. \end{matrix} \tag{6.1}$$

Now, according to (4.18), the AF periodic solutions at the FR–AF intersections are given by (4.17) at energies $e_\pm$:

$$\left.\begin{cases} u_j^+ = s\epsilon'\left(\frac{2v}{v-1}\right)^{\frac{1}{2}} \\ \quad \times \exp\left[\mathrm{i}\left(\boldsymbol{k}'\cdot\boldsymbol{R}_j + \left(b \pm \sqrt{1-v^2}\right)\tau - \phi'\right)\right] \\ u_j^z = \pm s\left(\frac{1+v}{1-v}\right)^{\frac{1}{2}} \end{cases}\right\} \qquad \begin{matrix} \phi' \in [0, 2\pi), \quad v \in [-1, 0] \\ j = 1, \ldots, \Lambda \\ \epsilon' \equiv \begin{Bmatrix} +1, & \text{if } v' \leqslant 0 \\ \epsilon_{\mathcal{A}(\mathcal{B})}, & \text{if } v' \geqslant 0 \end{Bmatrix}. \end{matrix} \tag{6.2}$$

Note that in the special case $v = -1$ we cannot use (4.17), but we derive (6.2) all the same, starting from (4.15) with $\theta = \frac{\pi}{2}$. Comparing (6.1) with (6.2), it only remains to find, in the case $v \neq 0$, the relation between $\boldsymbol{k}'$ and $\boldsymbol{k}$ so that

$$\exp[\mathrm{i}(\boldsymbol{k}\cdot\boldsymbol{R}_j - \phi)] = \epsilon' \exp[\mathrm{i}(\boldsymbol{k}'\cdot\boldsymbol{R}_j - \phi')]. \tag{6.3}$$

In view of the discussion in section 5, the constant phases ϕ, ϕ' must be equal and the wavevector of the two AF families is given by

$$\boldsymbol{k}' = \begin{Bmatrix} \widetilde{\boldsymbol{k}}, & \text{if } v' \in (0, +1] \\ \boldsymbol{k}, & \text{if } v' \in [-1, 0) \end{Bmatrix}. \tag{6.4}$$

It is important to keep in mind, though, that to label the AF families we only need to consider $\boldsymbol{k}'$ such that $v' \leqslant 0$ (or $v' \geqslant 0$).

We conclude that, for a general Bravais lattice, every pair of AF NLSW families bifurcates from a unique FR NLSW family. The momentum $\boldsymbol{k}'$ of the two AF families and the momentum $\boldsymbol{k}$ of the FR family are related according to (6.4). The FR families with $v(\boldsymbol{k}) \notin [-1, 0]$ display no FR–AF bifurcations. To visualize the approach to bifurcation along the AF families, we can plot the spin z-components of the two sublattices as functions of the energy (see figure 3). Two families of opposite momentum correspond to each curve in figure 3. Figures 3(a) and (b) also show the values of $\cos(\pi - \theta)$ in terms of the energy for the negative field $b = -0.9$ and for the large and small frequencies respectively (given that we

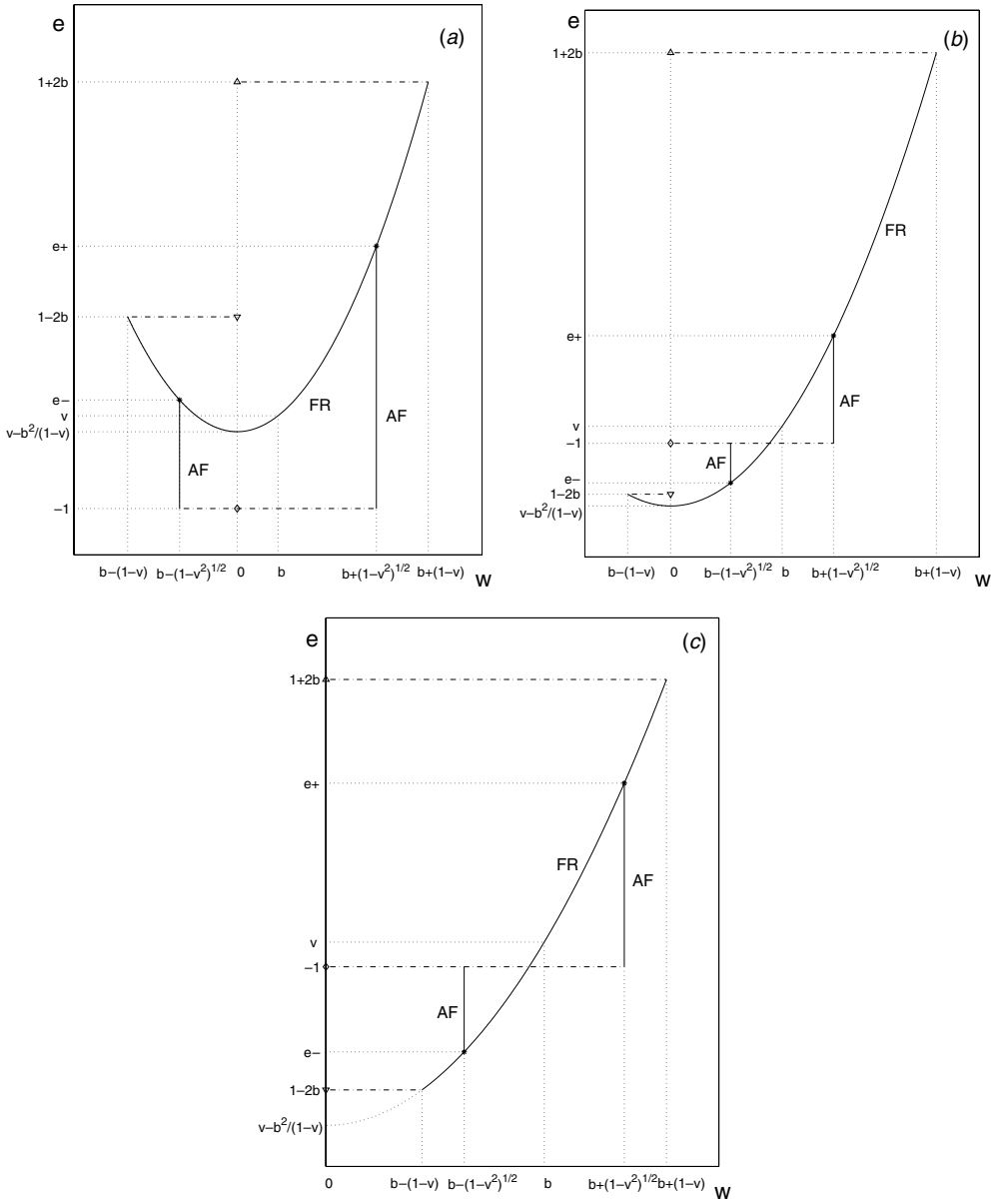

Figure 2. e–w plots of the NLSW solutions for $-1 < v < 0 < b$. The FR fixed point with all spins pointing along the positive (negative) z-axis is denoted by $\triangle$ ($\triangledown$). The AF fixed point, that is, the Néel stationary state (with even sublattice pointing either 'up' or 'down'), is denoted by $\Diamond$. The solid lines are the FR and AF e–w curves. The dashed-dotted lines signify bifurcations from fixed points. We use the asterisk to mark the FR–AF isochronous branching. Finally, the thin dotted lines help visualize certain points on the e–w curves. We distinguish the following cases: (*a*) $-1 < v < 0 < b < \sqrt{1-v^2}$ (*b*) $-1 < v < 0 < \sqrt{1-v^2} < b < 1-v$ (*c*) $-1 < v < 0 < 1-v < b$.

interchange solid and dashed line type). Also, it is worth noting that, according to the second equation in (6.2), the ordinates (spin angles) of the bifurcation points are independent of the magnetic field.

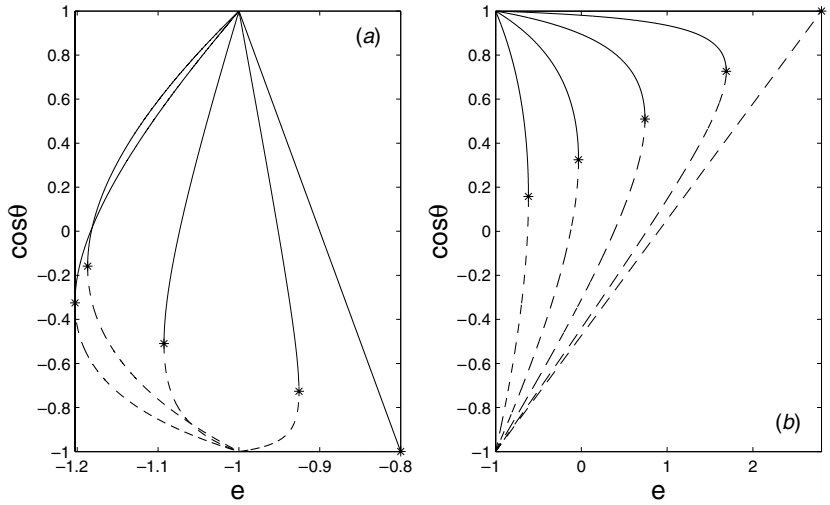

Figure 3. The Heisenberg chain of $L = 20$ sites under the influence of a magnetic field $b = 0.9$. Each solid (dashed) curve shows the behaviour of the z-component per spin length of the 'up' ('down') sublattice, as the energy e varies along a particular AF family. The FR–AF bifurcations are denoted by the asterisk. There are five distinct pairs of curves meeting at bifurcation points for (*a*) small frequencies; similarly for (*b*) large frequencies. These correspond to the different values of $|v| = \cos(\pi\alpha/10)$, $\alpha = 1, \ldots, 5$ where, in each plot, α increases from left to right.

Looking closer at the role of the latter in the FR–AF bifurcations, note that in the absence of an external field ($b = 0$), the two AF families have opposite frequencies and endpoints at the same energy, as one can also see in figure 2(*a*). Therefore, the FR–AF bifurcations for $b = 0$ are represented by the very same point on the E–T (energy–period) plot. On the other hand, with the introduction of a magnetic field, the resulting $z \to -z$ symmetry breaking induces a 'splitting' of this branching point of the *E–T* plot to two distinct ones.

7. Discussion

We presented in detail the various cases of NLSW families for the classical HM and studied the isochronous bifurcations between the FR and AF branches. Our analysis shows that, once the role of the wavevector $\boldsymbol{k}$ has been clarified, the FR–AF bifurcations can be described in the context of a general Bravais lattice and possibly long-range interactions, and in a way as simple as for a small spin ring. We have also allowed for longitudinal anisotropy as well as a uniform constant magnetic field along the line of anisotropy.

We would like to mention a number of ways in which one might want to extend further the ideas presented here. It is interesting to investigate numerically how the stability of periodic orbits evolves along a family. To the extent that the qualitative change of dynamics, in the vicinity of a bifurcation, surfaces at the linear level, one can characterize the FR–AF bifurcations in terms of the behaviour of the Floquet multipliers. We have already made a start in this direction, and our results will appear in [43]. Other possibilities include the extension of these ideas to the case of single-ion anisotropy which bends the AF families off the vertical line, and the study of 'off-shell' families of solutions, that is, generalized NLSWs for unequal spins [42].

Acknowledgments

The author would like to thank Professor Michel Baranger for bringing the Heisenberg model into focus and for reading this manuscript. He is also grateful to Pavlos Kazakopoulos and Dr Elefterios Lidorikis for helpful discussions. Finally, he wishes to acknowledge the Center for Theoretical Physics at MIT for granting financial support.

References

[1] Anderson P W 1959 New approach to the theory of superexchange interactions *Phys. Rev.* **115** 2–13
[2] White R M 1970 *Quantum Theory of Magnetism* (New York: McGraw-Hill)
[3] Yosida K 1996 *Theory of Magnetism* (Berlin: Springer)
[4] Levy L P 2000 *Magnetism and Superconductivity (Texts and Monographs in Physics)* (Berlin: Springer)
[5] Lieb E H and Mattis D 1962 Ordering energy levels of interacting spin systems *J. Math. Phys.* **3** 749–51
[6] des Cloizeaux J and Pearson J J 1962 Spin-wave spectrum of the antiferromagnetic linear chain *Phys. Rev.* **128** 2131–5
[7] Bonner J C and Fisher M E 1964 Linear magnetic chains with anisotropic coupling *Phys. Rev.* **135** 640A–58A
[8] Fröhlich J and Lieb E H 1978 Phase transitions in anisotropic lattice spin systems *Commun. Math. Phys.* **60** 233–67
[9] Haldane F 1982 Continuum dynamics of the $1-D$ Heisenberg antiferromagnet: identification with the $O(3)$ nonlinear sigma model *Phys. Lett.* A **93** 464–8
[10] Botet R, Julien R and Kolb M 1983 Finite-size scaling study of the spin-1 Heisenberg–Ising chain with uniaxial anisotropy *Phys. Rev.* B **28** 3914–21
[11] Parkinson J B and Bonner J C 1985 Spin chains in a field: crossover from quantum to classical behavior *Phys. Rev.* B **32** 4703–24
[12] Schulz H J 1986 Phase diagrams and correlation exponents for quantum spin chains of arbitrary spin quantum number *Phys. Rev.* B **34** 6372–85
[13] Affleck I and Lieb E H 1986 A proof of part of Haldane's conjecture on spin chains *Lett. Math. Phys.* **12** 57–69
[14] Affleck I, Kennedy T, Lieb E H and Tasaki H 1987 Rigorous results on valence-bond ground states in antiferromagnets *Phys. Rev. Lett.* **59** 799–802
[15] Horsch P and von der Linden W 1988 Spin-correlations and low lying excited states of the spin-$1/2$ Heisenberg antiferromagnet on a square lattice *Z. Phys.* B **72** 181–93
[16] Chakravarty D R N S and Halperin B I 1988 Two-dimensional quantum Heisenberg antiferromagnet at low temperatures *Phys. Rev.* B **39** 2344–71
[17] Neuberger H and Ziman T 1989 Finite-size effects in Heisenberg antiferromagnets *Phys. Rev.* B **39** 2608–18
[18] Manousakis E 1991 The spin-$1/2$ Heisenberg antiferromagnet on a square lattice and its application to the cuprous oxides *Rev. Mod. Phys.* **63** 1–62
[19] Kennedy T and Tasaki H 1992 Hidden symmetry breaking and the Haldane phase in $S = 1$ quantum spin chains *Commun. Math. Phys.* **147** 431–84
[20] White S R and Huse D A 1993 Numerical renormalization-group study of low-lying eigenstates of the antiferromagnetic $s = 1$ Heisenberg chain *Phys. Rev.* B **48** 3844–52
[21] Golinelli O, Jolicoeur T and Lacaze R 1994 Finite-lattice extrapolations for a Haldane-gap antiferromagnet *Phys. Rev.* B **50** 3037–44
[22] Yamamoto S 1995 Quantum Monte Carlo approach to elementary excitations of antiferromagnetic Heisenberg chains *Phys. Rev. Lett.* **75** 3348–51
[23] Dagotto E and Rice T M 1996 Surprises on the way from 1d to 2d quantum magnets: the novel ladder materials *Science* **271** 218–35
[24] Beard B B, Birgeneau R J, Greven M and Wiese U J 1998 The square-lattice Heisenberg antiferromagnet at very large correlation lengths *Phys. Rev. Lett.* **80** 1742–5
[25] Wang X, Qin S and Yu L 1999 Haldane gap for the $s = 2$ antiferromagnetic Heisenberg chain revisited *Phys. Rev.* B **60** 14529–32
[26] Leung K M, Hone D W, Mills D L, Riseborough P S and Trullinger S E 1980 Solitons in the linear chain antiferromagnet *Phys. Rev.* B **21** 4017–26
[27] Mikeska H J and Steiner M 1991 Solitary excitations in one-dimensional magnets *Adv. Phys.* **40** 191–356
[28] Daniel M and Amuda R 1995 Nonlinear dynamics of weak ferromagnetic spin chains *J. Phys. A: Math. Gen.* **28** 5529–37

[29] Daniel M, Porsezian K and Lakshmanan M 1994 On the integrability of the inhomogeneous spherically symmetric Heisenberg ferromagnet in arbitrary dimensions *J. Math. Phys.* **35** 6498–510
[30] Porsezian K 1997 Nonlinear dynamics of the radially symmetric and site dependent anisotropic Heisenberg spin chain *Chaos, Solitons Fractals* **8** 27–31
[31] Daniel M and Gutkin E 1994 The dynamics of a generalized Heisenberg ferromagnetic spin chain *Chaos* **5** 439–42
[32] Suhl H 1957 The theory of ferromagnetic resonance at high signal powers *J. Phys. Chem. Solids* **1** 209–27
[33] Bertotti G, Mayergoyz I D and Serpico C 2001 Spin-wave instabilities in large scale nonlinear magnetization dynamics *Phys. Rev. Lett.* **87** 217203
[34] Wang R W, Mills D L, Fullerton E E, Kumar S and Grimsditch M 1996 Magnons in antiferromagnetically coupled superlattices *Phys. Rev.* B **53** 2627–32
[35] Rakhmanova S, Mills D L and Fullerton E E 1998 Low frequency dynamic response and hysteresis in magnetic superlattices *Phys. Rev.* B **57** 476–84
[36] Rakhmanova S and Mills D L 1998 Intrinsic localized spin waves in classical one-dimensional spin systems: studies of their interactions *Phys. Rev.* B **58** 11458–64
[37] Roberts J A G and Thompson C J 1988 Dynamics of the classical Heisenberg spin chain *J. Phys. A: Math. Gen.* **21** 1769–80
[38] Mattis D C 1965 *The Theory of Magnetism (Harper's Physics Series)* (New York: Harper and Row)
[39] Balakrishnan R and Dhamankar R 1997 Exact nonlinear spin waves in some models of interacting classical spins on a one-dimensional lattice *Phys. Lett.* A **237** 73–9
[40] Aguiar M A M D, Malta C P, Baranger M and Davies K T R 1987 Bifurcations of periodic trajectories in non-integrable Hamiltonian systems with two degrees of freedom: numerical and analytical results *Ann. Phys.* **180** 167–205
[41] Negele J W 1982 The mean field theory of nuclear structure and dynamics *Rev. Mod. Phys.* **54** 913–1015
[42] Pantelidis L Off-shell nonlinear spin-wave solutions for the Heisenberg model in preparation
[43] Pantelidis L On the stability of the nonlinear spin waves of the Heisenberg model in preparation